



OPEN ACCESS

EDITED BY

Younseong Song,
Center for NanoImaging, Brigham and
Women's Hospital, United States

REVIEWED BY

Oleh Smutok,
Clarkson University, United States
Elsa Materon,
University of São Paulo, Brazil

*CORRESPONDENCE

Philippe C. Dixon,
✉ philippe.dixon@mcgill.ca

RECEIVED 31 October 2025

REVISED 11 January 2026

ACCEPTED 19 January 2026

PUBLISHED 13 February 2026

CITATION

Jlassi O, Hadid A, McDonald EG, Ding Q,
Phillipp C, Trottier A, Cheng MP, Papenburg J,
Libman M, Jensen D and Dixon PC (2026)
Predicting viral respiratory tract infections using
wearable biosensor monitoring during 3-
minute constant rate stair stepping tests.
Front. Sens. 7:1736869.
doi: 10.3389/fsens.2026.1736869

COPYRIGHT

© 2026 Jlassi, Hadid, McDonald, Ding, Phillipp,
Trottier, Cheng, Papenburg, Libman, Jensen
and Dixon. This is an open-access article
distributed under the terms of the [Creative
Commons Attribution License \(CC BY\)](#). The use,
distribution or reproduction in other forums is
permitted, provided the original author(s) and
the copyright owner(s) are credited and that the
original publication in this journal is cited, in
accordance with accepted academic practice.
No use, distribution or reproduction is permitted
which does not comply with these terms.

Predicting viral respiratory tract infections using wearable biosensor monitoring during 3-minute constant rate stair stepping tests

Oussama Jlassi¹, Amir Hadid¹, Emily G. McDonald²,
Qianggang Ding^{3,4}, Christopher Phillipp¹, Audrey Trottier¹,
Matthew P. Cheng⁵, Jesse Papenburg⁶, Michael Libman⁷,
Dennis Jensen¹ and Philippe C. Dixon^{1*}

¹Department of Kinesiology and Physical Education, Faculty of Education, McGill University, Montréal, QC, Canada, ²Department of Medicine, Division of General Internal Medicine, McGill University Health Center, Montréal, QC, Canada, ³Mila – Quebec AI Institute, Montréal, QC, Canada, ⁴Department of Computer Science and Operations Research, Université de Montréal, Montréal, QC, Canada, ⁵Department of Medicine, Research Institute of McGill University Health Center, Divisions of Infectious Diseases and Medical Microbiology, Infectious Diseases and Immunity in Global Health Program, Montréal, QC, Canada, ⁶Department of Pediatrics, Division of Pediatric Infectious Diseases, Montreal Children's Hospital, McGill University Health Centre, Montréal, QC, Canada, ⁷Research Center of the Sainte-Justine University Hospital, Montréal, QC, Canada

Background: Viral Respiratory Tract Infections (VRTIs) are a major public health threat. Early detection and preventive measures are key to controlling their spread. Current machine learning approaches often depend on symptom onset, costly equipment, trained personnel, and slow results. This study aims to evaluate whether a machine learning algorithm using physiological data from wearable biosensors during a constant-rate stair-stepping task (3-min test, 2-min recovery) can predict inflammation levels, and to identify the most predictive indicators of VRTI.

Methods: 55 Healthy participants (27 males and 28 females) aged 18–59 years, were recruited and inoculated with a live influenza vaccine to induce an immune response, assessed via changes in circulating inflammatory biomarkers. Physiological markers, including breathing rate and heart rate, during a series of clinically controlled stair tests, were monitored by a wearable biosensor. These data were collected to develop a prediction model using gradient-boosting machine learning algorithms combined with hyperparameter tuning and a leave-one-subject-out method to train the models.

Results: The study developed a predictive model that accurately estimates inflammation levels in individuals. Features from heart rate variability (HRV) showed the greatest potential, with 70% sensitivity and 77% specificity, and physiological markers from controlled stair tests correlated with VRTI-related inflammatory responses.

Impact: The prediction model linked to stair-stepping tests offers clinicians and the public a tool for self-monitoring and early intervention. Using machine learning and physiological markers, especially HRV features, it can help guide timely treatments and reduce the impact of future outbreaks.

KEYWORDS

3-min constant rate stair stepping test, early detection, heart rate variability, machine learning, physiological markers, viral respiratory tract infections, wearable biosensors

1 Introduction

Viral respiratory tract infections (VRTIs), such as COVID-19 and influenza, remain major public health concerns due to their rapid transmission and potential for severe outcomes, including death. As of July 2024, Canada has reported 4,562,906 COVID-19 cases and 38,340 deaths (of Canada, 2023), highlighting the urgent need for effective early detection strategies. Early identification of VRTIs can enable timely interventions and help prevent widespread transmission. Traditional detection methods rely on molecular testing, including antigen assays, isothermal nucleic acid amplification, and polymerase chain reaction (PCR), which is considered the gold standard for COVID-19 detection (Shen et al., 2020). For instance, Lu et al. (2021) evaluated commercially available rapid PCR systems such as FilmArray (BioFire Diagnostics Inc., United States) that detect influenza A and B, and respiratory syncytial virus (RSV), reporting sensitivities of 97.1% and specificities of 99.3%. While accurate, these approaches require specialized equipment, trained personnel, and often provide delayed results, limiting their practicality for real-time early detection. Machine learning (ML) has emerged as a promising tool for VRTI detection. Narin et al. (2021) proposed an automatic COVID-19 detection method using chest X-ray images and deep convolutional neural networks (InceptionV3), achieving 90.6% sensitivity and 96.0% specificity. Similarly, Quer et al. (2020) developed ML models based on resting heart rate, sleep, and activity metrics, obtaining an area under the curve (AUC) of 0.72, while a symptom-only model reached an AUC of 0.80. Several recent studies have focused on symptom-based ML approaches: one analyzed self-reported changes in smell and taste to predict COVID-19 diagnosis with an AUC of 0.65 (Li et al., 2023), another modeled temporal patterns of patient-reported symptoms to detect RSV in pediatric patients with an AUC of 0.811 (Kawamoto et al., 2024), and a third evaluated influenza detection using self-reported symptom data, achieving an AUC of 0.74 (Farooq et al., 2024). However, models

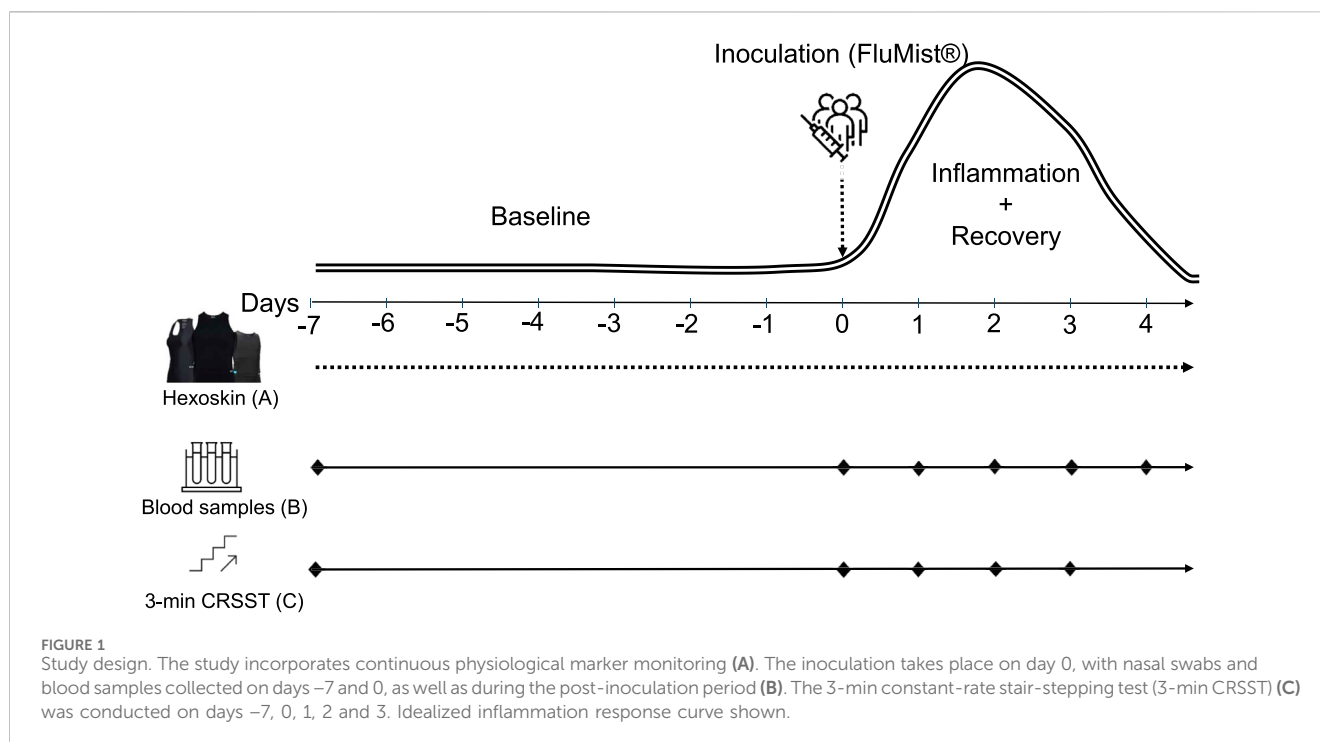
relying solely on patient-reported symptoms remain limited in detecting presymptomatic or asymptomatic infections. Biological markers (biomarkers) offer an objective measure of the host immune response, often rising several hours before symptom onset (Mayeux, 2004). Key biomarkers associated with inflammation include monocyte chemoattractant protein 1 (MCP-1), interleukins (IL-6, IL-8, IL-10, IL-15), interferon gamma (IFN γ), interferon gamma-induced protein 10 (IP-10), and tumor necrosis factor alpha (TNF α) (McClain et al., 2015; Davey et al., 2013; Lee et al., 2011; Chi et al., 2013; Peiris et al., 2004; Monteerarat et al., 2010). Furthermore, heart rate variability (HRV) has been inversely correlated with inflammation (Williams et al., 2019; Haarala et al., 2011; Hasty et al., 2021; Timothy et al., 2015), suggesting that wearable physiological monitoring may provide early warning signals of VRTIs. Building on this rationale, we previously demonstrated in the WE SENSE study (Hadid et al., 2023) that combining wearable sensor data (including heart rate, breathing rate, and activity) with systemic inflammatory biomarkers allows machine learning algorithms to accurately predict systemic inflammatory surges following low-grade influenza exposure, even in asymptomatic individuals. Specifically, models using Oura ring night-time data achieved a real-time Receiver Operating Characteristic Area Under the Curve (ROC-AUC) of 0.73 and a 24-h tolerance ROC-AUC of 0.89, outperforming symptom-based detection (Hadid et al., 2025). These findings confirmed that integrating objective physiological and immunological measurements can enhance early VRTI detection. In the present study, we extend this approach by investigating the utility of a controlled exercise protocol for early inflammation detection. Specifically, we aim to (1) evaluate whether a 3-min constant-rate stair-stepping task (3-min CRSST) can predict the level of systemic inflammation using ML algorithms and wearable biosensors, and (2) identify the most informative sensor-derived features associated with VRTI-related inflammation. This work builds on our prior findings (Hadid et al., 2023; Hadid et al., 2025) and explores practical strategies for early, objective detection of VRTIs.

2 Materials and methods

2.1 Participants

We recruited 55 healthy adults (27 males and 28 females aged 18–59 years). Exclusion criteria were pre-existing respiratory tract infections or other underlying health conditions. Additionally, we only recruited participants who did not intend to receive a COVID-19 or seasonal influenza vaccine during the study period, and

Abbreviations: VRTIs, Viral Respiratory Tract Infections; HRV, Heart Rate Variability; PCR, Polymerase Chain Reaction; RSV, Respiratory Syncytial Virus; ML, Machine Learning; AUC, Area Under the Curve; MCP-1, Monocyte Chemoattractant Protein 1; IL, Interleukins; IFN γ , Interferon gamma; IP-10, Interferon gamma-Induced Protein 10; TNF α , Tumor Necrosis Factor alpha; ROC-AUC, Receiver Operating Characteristic Area Under the Curve; HR, Heart Rate; bpm, Beats per minute; BR, Breathing Rate; rpm, Respirations per minute; MV, Minute Ventilation; RRI, R-wave to R-wave Interval; ECG, Electrocardiogram; 3-min CRSST, 3-min Constant Rate Stair Stepping Test; LAIV, Live Attenuated Influenza Vaccine; IRS, Immune Response Score; CoV, Coefficient of Variance; XGBoost, eXtreme Gradient Boosting; MSE, Mean Squared Error; RMSSD, Root Mean Square of Successive Differences; NNI, Normal-to-Normal Interval; METs, Established Metabolic Equivalents; CI, Confidence Interval.



participants had to be clear of any other inflammation within 7 days prior to the start of the study. Data were collected from December 2021 to February 2022. Participants were recruited through word-of-mouth and posted advertisements in Montreal, Canada. Further details about the inclusion, exclusion, and withdrawal criteria are provided in the study protocol (Hadid et al., 2023).

2.2 Study design and data collection

The study period lasted 12 days and was divided into two distinct phases: the pre-inoculation period (considered as day -7 to day 0) and the post-inoculation period (day 0 to day 4). Starting from day -7, participants continuously wore a Astroskin (10 participants)/Hexoskin (45 participants) garment (Carré Technologies, Inc. Montreal, Canada) to monitor their physiological markers (Figure 1A). Blood samples were also collected (Figure 1B), 3-min CRSST followed by 2 min of recovery was conducted (Figure 1C). The Astroskin/Hexoskin garment was used to collect the following physiological markers relevant to respiratory health:

- Heart Rate (HR): The number of heartbeats per minute (bpm)
- Breathing Rate (BR): The number of respirations per minute (rpm)
- Minute Ventilation (MV): The total volume of air breathed in a minute, derived from the breathing rate and the tidal volume, which is the volume of air inspired in the last inspiration (mL/minute)
- R-wave to R-wave Interval (RRI): The time duration between two consecutive heart beats on an electrocardiogram (ECG) (seconds)

The data format of the measured physiological markers is a 1-D array counting 300 rows (1 data point every second) per physiometer per visit. Each data point is an integer number for HR, BR, and MV, and a floating point value for RRI. Although the Astroskin shirt also measures blood oxygen concentration, we limited analyses to signals that were common to both garments (the exact same raw data is provided by both biosensors). Prior validation studies have demonstrated that both devices offer highly comparable and reliable measurements for the physiological markers considered in this study (Harbour et al., 2021; Montes et al., 2018; Smith et al., 2019). The choice of these devices was driven by their non-invasive design, ability to capture continuous multi-channel physiological data, and validated accuracy in measuring cardiac and respiratory signals during physical activity and recovery. On day 0, blood samples, and a 3-min CRSST at 30 steps/min for all participants were performed to provide additional baseline data and assess participants' physiological responses during exertion. Participants were then inoculated with a live attenuated influenza vaccine (LAIV): FluMist® (Carter and Curran, 2011). The post-inoculation period (5 days) involved daily blood sample collection to monitor the participants' response to the inoculated influenza vaccine. Participants performed the 3-min CRSST three additional times during the post-inoculation period (days 1, 2 and 3).

2.3 Calculating the immune response score

Blood samples facilitated the measurement of biomarkers and immune-related factors, aiding in identifying baseline levels and subsequent changes induced by the influenza vaccine. The inflammation level was obtained by calculating the immune response score (IRS) which is the objective of our prediction

TABLE 1 Overview of the biomarkers analyzed in this study, including their biological definitions and primary roles in immune and inflammatory responses.

Biomarker	Definition
IFN γ	Interferon-gamma (IFN γ) is a cytokine that plays a crucial role in the immune response to viral infections and various immune system functions
IL-6	Interleukin-6 (IL-6) is a proinflammatory cytokine involved in the regulation of immune responses and acute-phase reactions
IL-8	Interleukin-8 (IL-8) is a chemokine that attracts and activates neutrophils, playing a key role in the inflammatory response
IL-10	Interleukin-10 (IL-10) is an anti-inflammatory cytokine that helps regulate and limit immune responses
IL-15	Interleukin-15 (IL-15) is involved in immune system functions, including the development and activation of T and natural killer cells
IP-10	Interferon-gamma-induced protein 10 (IP-10) is a chemokine that recruits immune cells to sites of infection and inflammation
MCP-1	Monocyte chemoattractant protein-1 (MCP-1) is a chemokine that attracts monocytes to sites of injury and infection
TNF α	Tumor necrosis factor-alpha (TNF α) is a proinflammatory cytokine that plays a key role in the body's response to infection and inflammation

TABLE 2 Comparison of machine learning model performance using non-normalized IRS (mean squared error).

Model	MSE
XGBoost	0.1552
Random forest	0.1767
SVR	0.1696
Linear regression	0.1800

Analysis performed on the top model (HRV, during the first minute of recovery).

model. This score is composed of the mean value of 8 measured biomarkers (IFN γ , IL-6, IL-8, IL-10, IL-15, IP-10, MCP-1, and TNF α) during each visit (Equation 1). A detailed definition of each biomarker is presented in Table 1. These biomarkers were chosen due to their ability to detect inflammation in the host immune system (McClain et al., 2015; Davey et al., 2013; Lee et al., 2011; Chi et al., 2013; Peiris et al., 2004; Monteerarat et al., 2010). We then used 4 IRS scores obtained from the baseline period (2 scores per visit), to calculate the IRS' coefficient of variance (CoV) for each participant (Equation 2), allowing us to assess the individual variation of the IRS values. We used these CoV values to apply a 0-CoV normalization (Equation 3) to the original IRS. By normalizing the IRS values, the individual baseline variations among all participants are eliminated, thus, providing generalizable scores of inflammation levels. Additional analyses using the raw IRS scores (without normalization) were performed to assess the impact of this step (Table 2).

2.4 Physiological parameter monitoring (stair test)

The stair test consists of stepping for 3 min (with a consistent pace of 30 steps/minute) up and down a step having a height of 20 cm (Hadid et al., 2023). We chose this controlled clinical test as it's been previously used to uncover information about a participant's physiological response to exercise-induced stress (Li et al., 2021; Elsaid, 2011; Kieu et al., 2020; Lee et al., 2019). Following the test, participants recovered in a seated position for 2 min. Physiological markers were monitored during the entire session.

Although oxygen consumption was not directly measured during the 3-min CRSST, exercise intensity can be estimated using the American College of Sports Medicine (ACSM) stepping equations. Based on the fixed stepping rate (30 steps/min), step height (20 cm), and individual body mass, the ACSM equations allow estimation of oxygen consumption and corresponding metabolic equivalents (METs) at the end of the CRSST. These estimates indicate that the CRSST elicits a moderate-intensity workload, approximately 5–7 METs, corresponding to 50%–70% of maximal oxygen uptake (VO $_{2max}$) in healthy adults (Lewthwaite et al., 2020).

2.5 Data processing and feature extraction

First, the 5-min period of interest (stair test and recovery) was segmented based on annotated timestamps, resulting in 238 visits having 4 signal data files per visit and 300 data points (integer numbers) per signal (Figure 3A). We then plotted all the sensor data for each visit to assess the signal quality and identify missing or noisy segments through a visual inspection (Figure 3B). Exemplars of noisy and typical heart rate signals are shown in Figure 2. During this step, data were removed due to noisy signals from BR (24 visits), missing or noisy HR signal (49 visits), noisy MV signals (3 visits), and missing or noisy RRI signal (68 visits). Next, we performed data cleaning. This involved identifying inconsistencies and errors in the dataset that were flagged by Hexoskin's systems and the data cleaning protocols (detailed in Table 3 (Lewthwaite and Jensen, 2021; Blackie et al., 1991; Foll et al., 2021) and Figure 3C). The data points having such inconsistencies and errors are discarded from the record of the concerned visit (n = 10). Finally, we performed artifact removal for the RRI data following 3 rules (Acar, Karlsson and Malik rules) which resulted in excluding 4 visits. (Foll et al., 2021) (Figure 3D). It is worth noting that some visits met multiple exclusion criteria. The final number of remaining visits is 170. We extracted the HRV features during the first minute of recovery using the Flirt Python package (Foll et al., 2021). Flirt offers tools and algorithms specifically designed for extracting HRV-related features from the RRI signal, including statistical (e.g., min, max, mean), time-domain (e.g., skewness, kurtosis, number of peaks), and frequency-domain features (e.g., low frequency to high frequency ratio) (Figure 3E). Furthermore, we calculated

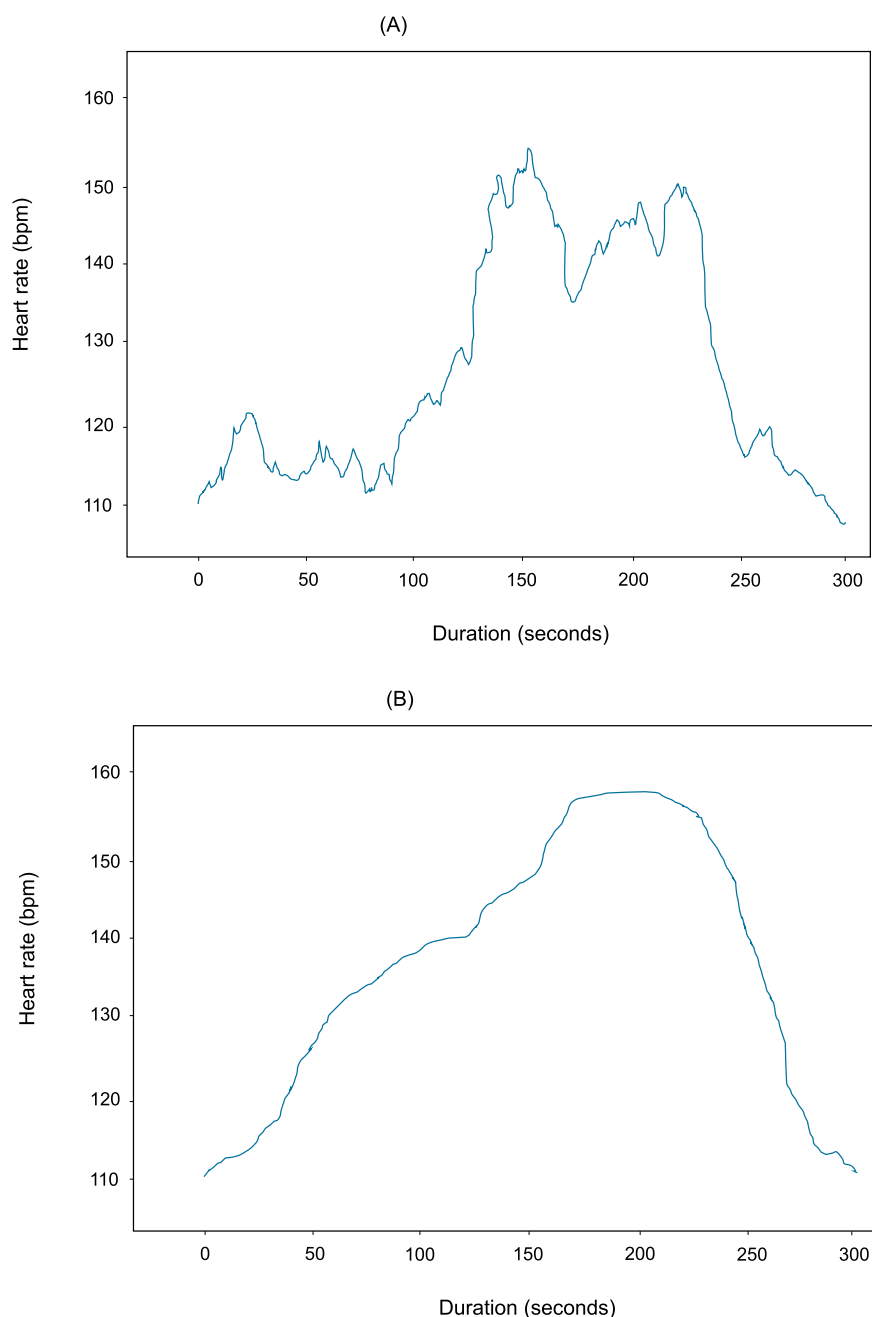


FIGURE 2 Visual inspection of the data during a 3-min constant rate stair stepping test (3-min CRSST). The top panel (A) illustrates a noisy or artifact-prone signal, whereas the bottom panel (B) shows a typical heart rate pattern reflecting normal physiological response. Abbreviations: bpm (beats per minute).

additional features to further enhance the analysis (Figure 3F). These features specifically targeted the BR, HR as well as the MV signals, and included the increase or decrease from the baseline during specific time intervals of the stair test, such as minutes 0 to 3 and 3 to 4 (Equation 4). An AUC feature was also calculated (using the Trapez function provided in the Numpy Python package (Developers, 2025)) for the 3 min of activity and the subsequent minute of recovery. A full list of features is provided in Table 4. Finally, we concatenated the cleaned data, extracted and calculated features, and consolidated all relevant information for a particular visit into a cohesive record. Afterwards, we merged all visits together resulting

in a final dataset having 170 rows (visits) and 40 columns (39 features and the corresponding IRS score for each visit) (Figure 3G).

2.6 Machine learning model development

Selecting an appropriate model for our task is a critical step. Our objective was to predict the IRS using a combination of physiological features obtained from wearable garment biosensors, making it a regression task. A Gradient Boosting algorithm [XGBoost (Chen

TABLE 3 Rules applied for cleaning physiological signal data before analysis.

Signal	Cleaning rules Lewthwaite and Jensen (2021), Blackie et al. (1991), Foll et al. (2021)
BR	Keep data points where the BR quality flag is 0 or 2
	Discard data points where BR is outside the range [4, 60] rpm
MV	Keep data points where MV is under 160,000 mL/min
RRI	Discard data points where RRI quality is 128
	Discard data points where RRI is outside the range [0.25, 2] seconds

Abbreviations: BR (breathing rate), rpm (respirations per minute), MV (minute ventilation), RRI (R wave to R wave interval). Data quality flags 0, 2 and 128 correspond to “good quality respiration”, “abdominal channel disconnected” (we can use the thoracic channel alone), and “unreliable RRI, signal”, respectively (Inc, 2023).

and Guestrin, 2016)] was selected due to its ability to model complex relationships, handle missing data, and its robust performance (Chen and Guestrin, 2016). We now describe the steps taken in our machine learning model development pipeline in order to predict the inflammation response score. First, data were split into train and test sets while keeping the number of visits pre and post-inoculation balanced in both sets. Five randomly selected participants were kept in the test set, and the remaining participants ($n = 50$) were included in the train set (Figure 6A) which will be used to train and tune the ML models. Next, we applied filter methods to the train set to reduce features and improve model performance (Figure 6B). We removed duplicate features, features with a variance lower than 0.01 across the dataset (poor predictive potential since these features are nearly invariant across inflammation states), and highly correlated features (correlation threshold, $r > 0.8$). Finally, we employed hyperparameter tuning to optimize our machine learning model’s performance. Specifically, we used GridSearchCV from the Scikit-learn library to systematically search through a predefined hyperparameter grid that included “max_depth”, “learning_rate”, “n_estimators”, and “alpha”. GridSearchCV performed multi-dimensional tuning, exploring various combinations of these hyperparameters, rather than tuning one hyperparameter at a time. GridSearchCV essentially performed an exhaustive search, trying every possible combination of hyperparameters defined in our grid to identify the combination that resulted in the least mean squared error (MSE) of the predicted IRS. The grid search approach was implemented with a 3-fold cross-validation to reduce the risk of overfitting (Figure 6C). A 3-fold cross-validation when tuning the hyperparameters means that the train data is split into 3 approximately equal parts. The grid search algorithm iteratively uses each fold as a testing set while the remaining two folds are used as the training set. This process is repeated three times, with each fold serving as the testing set exactly once. Table 5 presents the hyperparameters, the ranges, the final tuned value and the step size during the tuning process.

2.7 Machine learning model training and evaluation

We trained and tested models using a leave-one-subject-out strategy due to the limited number of data points (Figure 4). This

approach involved training on the combined train data ($n = 50$ participants for training which corresponds to 153 visits) and the test participants’ data for 5 iterations ($n = 5$ participants for testing, 16 visits), excluding one participant during each iteration. Specifically, we use the 50 (train) + 4 (test) participants data to train the model and we test its performance on the left out participant from the test set and we repeat that with each test participant. To assess model performance, mean and standard deviation of performance metrics (across the 5 test participants) are reported. We developed 8 models to assess the predictive potential of different feature sources. For the BR, HR, MV signals, we developed 2 models based on features extracted from the 3 min of activity and the first minute of recovery, respectively. The model based on HRV features was only generated for the recovery period since HRV analysis is mainly relevant during rest/recovery (Boullosa et al., 2014; Kannankeril et al., 2004; Stanley et al., 2013; Goldberger et al., 2006). Additionally, we trained a model based on the features derived from the combined signals. We evaluated the model’s performance using the MSE values of the predicted IRS (Figure 6E), then, we derived a binary outcome from the predicted values by setting a threshold to 0, classifying participants as no inflammation ($IRS \leq 0$) or high inflammation ($IRS > 0$) (Figure 5). This binary outcome enabled the evaluation of model performance via classification-related metrics (Figure 6G), including accuracy, sensitivity, specificity, precision, and AUC, which is the primary metric we used to evaluate the classification performance. The effect of varying thresholds in the range [-0.3, 0.3] is explored.

3 Results

3.1 Overview

The XGBoost models were able to predict the IRS based on features derived from the wearable sensors (Table 6). Models trained on the activity period (3 min of stair activity) achieved a maximum AUC of 0.66, the highest one was trained on HR features only. Models trained on the first minute of recovery achieved AUC scores of 0.43, 0.60, 0.69 and 0.73 (95% confidence interval CI: 0.70–0.77) for the BR, HR, MV, and HRV feature sets respectively. The highest performing model (recovery, HRV, AUC = 0.73) achieved a sensitivity of 0.7 (95% CI: 0.66–0.74), a specificity of 0.77 (95% CI: 0.73–0.81), and a precision of 0.75.

3.2 A closer look at the best-performing model

Further details related to the model with the strongest performance (recovery period, HRV, AUC = 0.73) are now presented. The model comprises 8 features (see Table 7; Figure 7 for a description of each feature and relative feature importance, respectively). Feature importance is a measure that quantifies the contribution of each input feature to the predictive performance of the model. It helps us understand which features have the most significant influence on the model’s predictions. XGBoost measures feature importance by computing the gain achieved from each

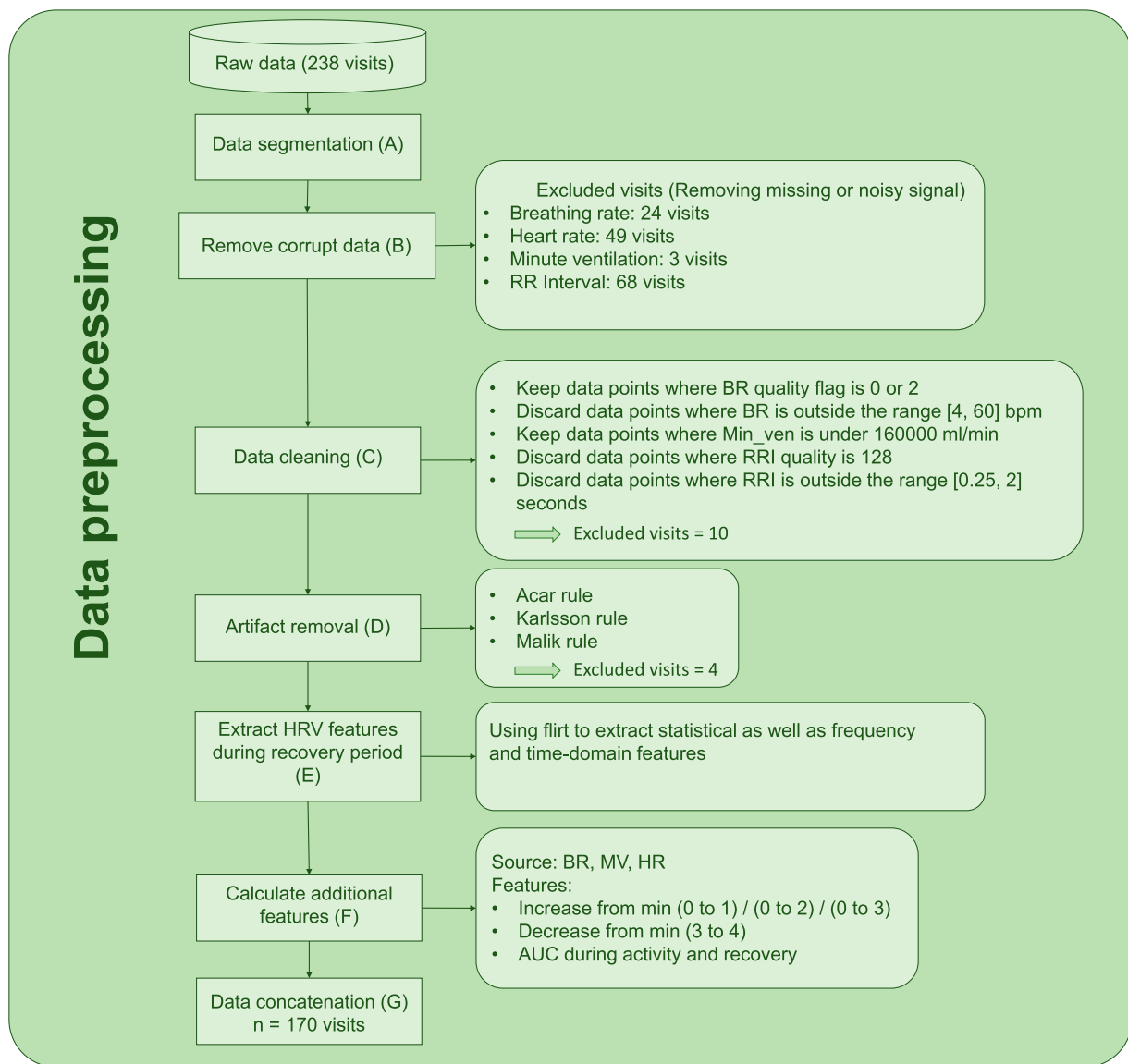


FIGURE 3 Diagrammatic representation of the data preprocessing approach. Raw data are segmented (A), inspected (B), cleaned (C), and artifacts are removed (D). Afterwards, features are calculated and concatenated (E,F,G). Abbreviations: HRV (Heart Rate Variability), RRI (R-wave to R-wave Interval), BR (breathing rate), bpm (beats per minute), HR (heart rate), MV (minute ventilation), AUC (area under the curve).

feature across all trees in the model. The gain represents the improvement in accuracy or reduction in loss resulting from a particular feature when used in a split decision within the trees. Features contributing to higher gain values are considered more important. In (Equation 5), the gain is calculated for each feature as it is used in each decision tree for splitting. The importance score for a feature is then determined by aggregating the gains across all trees, normalizing these values by the total sum of gains in the model.

3.3 Effect of binary conversion threshold on model performance

For the best model, the binary threshold was varied over the interval [-0.3, 0.3] in steps of 0.1 which allows to obtain the ROC-

AUC curve (Figure 8) (note that we cannot generate such curve automatically using Scikit Learn’s pre-existing methods since this is a regression task that was later converted to a classification task). Increasing thresholds led to maximizing specificity while decreasing thresholds maximized sensitivity (Table 8). Figure 8 is the corresponding ROC-AUC curve.

4 Discussion

4.1 Summary

This study aimed to assess the potential of wearables for early detection of systemic inflammation following exposure to a low-grade VRTIs using machine learning algorithms and data collected

TABLE 4 List of extracted features with their definitions and corresponding sources.

Feature name	Definition	Source
signal_inc_0_1	Difference of the signal from minute 0 to minute 1	Equation 4
signal_inc_1_2	Difference of the signal from minute 1 to minute 2	Equation 4
signal_inc_2_3	Difference of the signal from minute 2 to minute 3	Equation 4
signal_dec_3_4	Difference of the signal from minute 3 to minute 4	Equation 4
signal_auc_3	Area under the curve of the signal during the 3 min of activity	Numpy
signal_auc_3_4	Area under the curve of the signal during the first minute of recovery	Numpy
rmssd	Magnitude of the differences between consecutive heartbeats	Flirt
lf_hf_ratio	Low frequency to high-frequency ratio	Flirt
std_hr	Standard deviation of the heart rate	Flirt
peaks	Number of RRI peaks	Flirt
n_above_mean	Number of RRI peaks above the mean	Flirt
skewness	Skewness (asymmetry) of the data distribution	Flirt
range_nni	max (NN intervals) – min (NN intervals)	Flirt
kurtosis	Kurtosis of the data distribution	Flirt
sdnn	Standard deviation of the NNI	Flirt
cvnni	Coefficient of variation of the NNI	Flirt
mean_hrv	Heart rate variability mean value	Flirt
min_hrv	Heart rate variability minimum value	Flirt
max_hrv	Heart rate variability maximum value	Flirt
vlf_hrv	Very low-frequency power	Flirt
lf_hrv	Low-frequency power	Flirt
hf_hrv	High-frequency power	Flirt
lineintegral	Area under the curve of the heart rate variability	Flirt
iqr	Dispersion of the heart rate variability within the middle half of the data	Flirt
entropy	Entropy of the heart rate variability	Flirt
median_nni	Median of NN intervals	Flirt
mean_nni	Mean of NN intervals	Flirt

Signal can be heart rate, breathing rate, or minute ventilation. Abbreviations: RRI (R-wave to R-wave Interval), rmssd (root mean square of successive differences), NNI (Normal-to-Normal Interval).

TABLE 5 Tuned hyperparameters and their corresponding search ranges, meanings, and final selected values.

Hyperparameter	Range	Meaning	Tuned value	Step size
Alpha	0.5 to 0.6	Controls the regularization term in the model	0.5	0.1
Learning rate	0.01 to 1	Determines the step size at each boosting iteration, influencing the impact of each tree on the final prediction	0.1	0.01, 0.1, 0.5, 0.8, 1
Max depth	50 to 150	Limits the depth of each decision tree in the ensemble, preventing overcomplexity and reducing overfitting	50	10
N Estimators	50 to 100	Specifies the number of boosting rounds, representing the number of decision trees in the ensemble	50	10

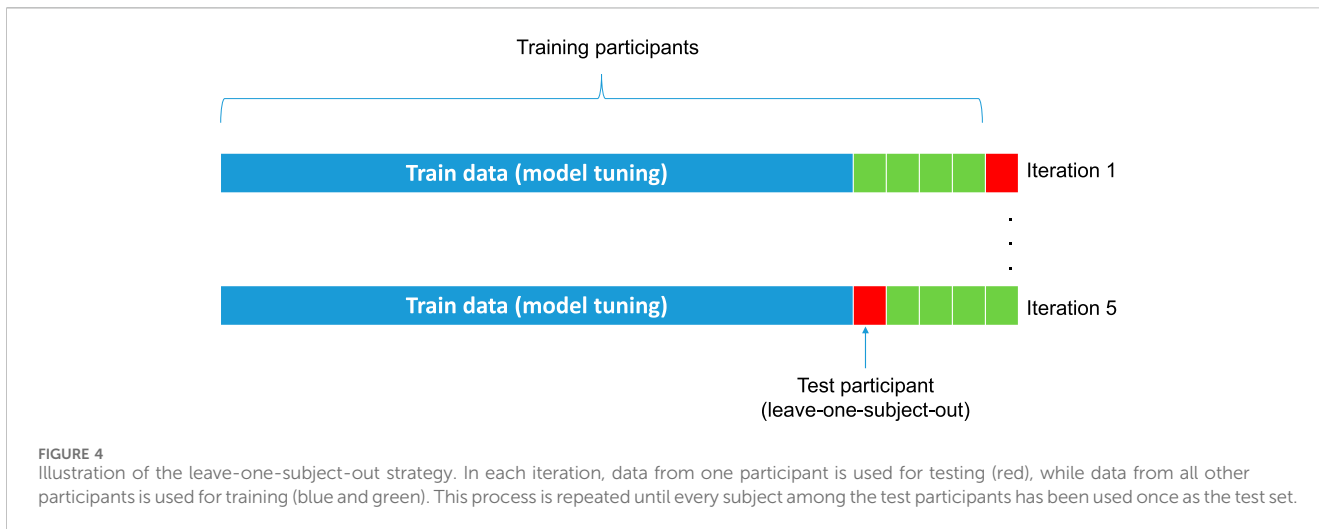


FIGURE 4 Illustration of the leave-one-subject-out strategy. In each iteration, data from one participant is used for testing (red), while data from all other participants is used for training (blue and green). This process is repeated until every subject among the test participants has been used once as the test set.

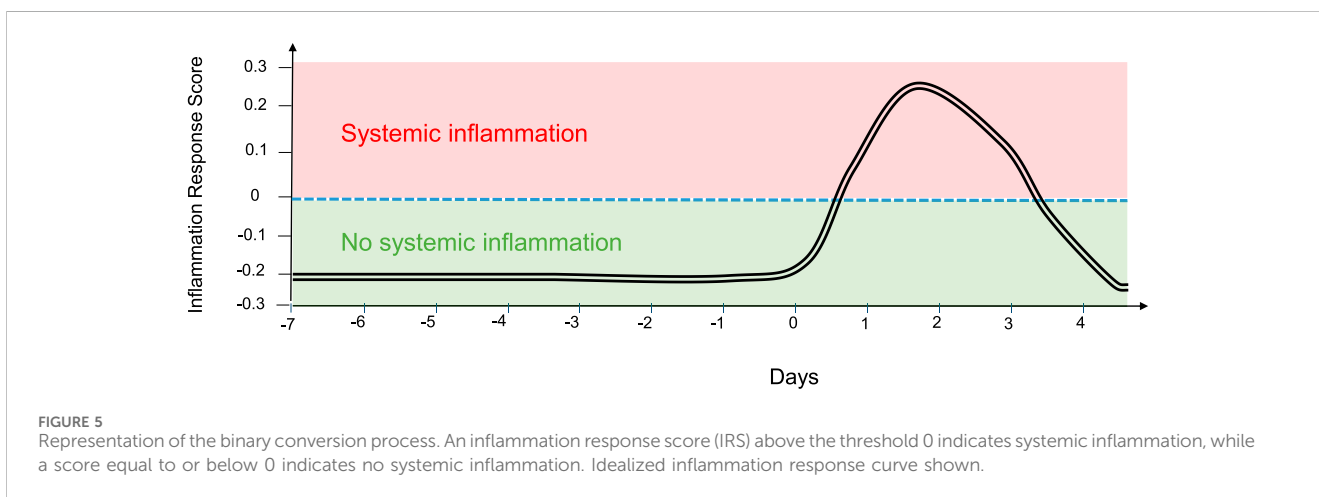


FIGURE 5 Representation of the binary conversion process. An inflammation response score (IRS) above the threshold 0 indicates systemic inflammation, while a score equal to or below 0 indicates no systemic inflammation. Idealized inflammation response curve shown.

during a controlled physical exercise (3-min CRSST). The model was able to predict the inflammation level using features derived from the wearable device. We were able to obtain the highest predictive ability using HRV features during the first minute of recovery after the 3-min CRSST.

4.2 Study design

The study design encompassed a structured timeline and a series of carefully planned visits and procedures. Even though moderate symptoms associated with viral replication are anticipated after the LAIV inoculation, we expected the participants’ immune systems to have a similar response as if exposed to mild influenza. The choice of the number of days pre-inoculation is justified by the fact that we wanted to establish a general baseline by capturing the most truthful trend within the participants’ daily lifestyle since a person’s physiological activity is not the same during all days of the week. Additionally, the choice of exactly 5 days post-inoculation is due to the fact that we wanted to capture all physiological states (no inflammation, high inflammation), especially the peak of

inflammation, which is estimated to happen during the first 4 days after inoculation (McClain et al., 2015). Additionally, the use of the Astroskin/Hexoskin biosensor is backed up by its ability to ensure a non-invasive and convenient solution for collecting real-time data, allowing for a comprehensive assessment of participants’ respiratory and cardiac variables throughout the study.

4.3 Effect of features on model performance

In line with our second objective, we demonstrated that features derived from different data sources have different predictive abilities. The model utilizing BR features during the activity period exhibited limited performance. Similarly, the MV during the activity period also displayed relatively lower performance metrics. However, the model trained on HR features during the activity period performed better than the other features in the same period. In contrast, models focused on the recovery period based on BR and MV features showed improvement compared to their activity-based counterparts. Notably, the MV features during the recovery period exhibited higher AUC and specificity, suggesting its potential relevance in

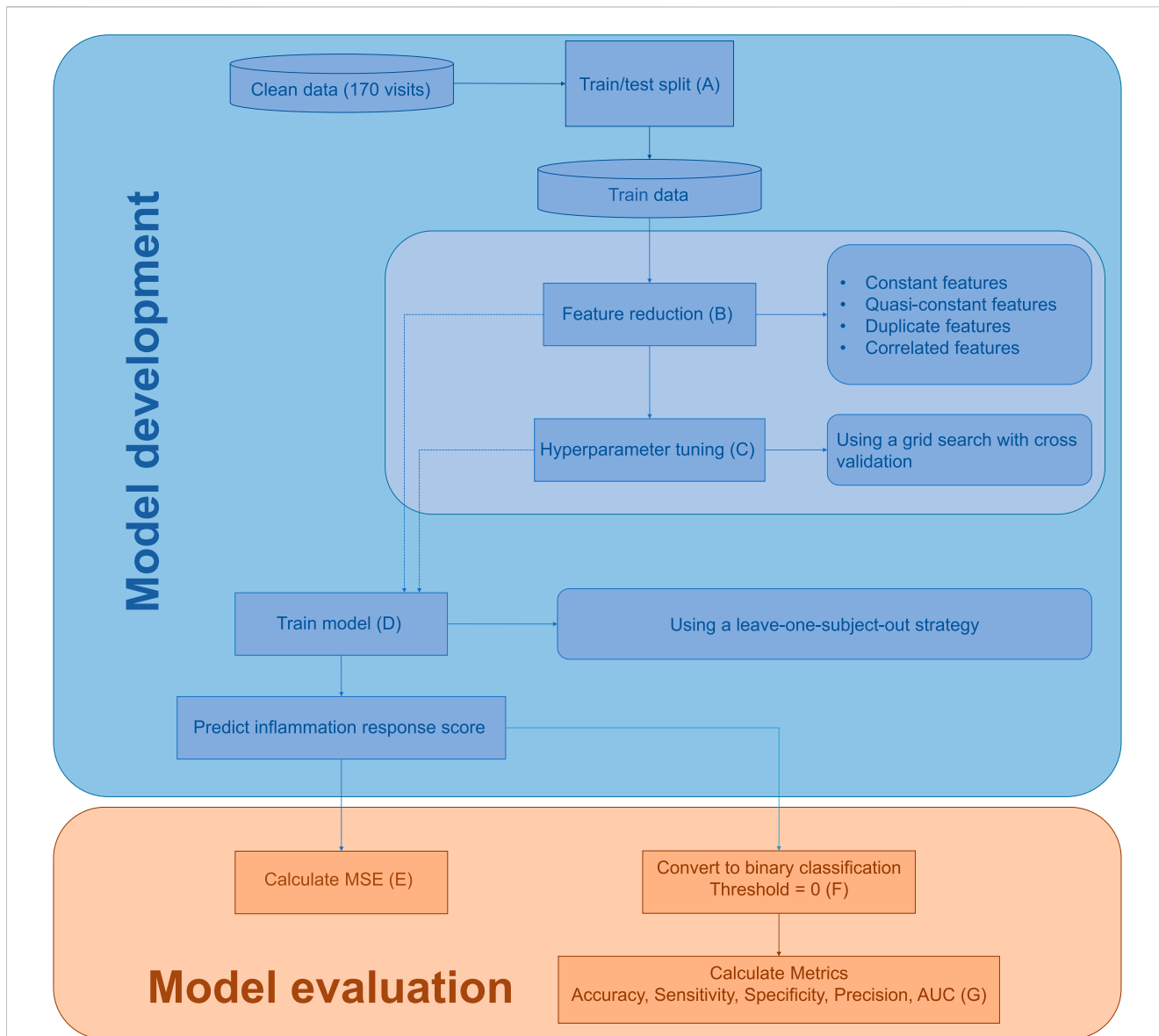


FIGURE 6 Model development and evaluation. Steps taken during the model development and evaluation phase are shown. Abbreviations: MSE (Mean Squared Error), AUC (Area Under the Curve).

predicting systemic inflammation due to VRTIs during recovery periods. Moreover, the model trained on HRV during the first minute of recovery revealed highest sensitivity, precision, and AUC values among the analyzed features. Finally, the model using the combined features derived from the HR, BR, MV, and RRI signals demonstrated poor performance metrics. These results demonstrate that HRV features are particularly important in enhancing the model’s predictive performance. These findings are aligned with previous research (Boullosa et al., 2014; Kannankeril et al., 2004; Stanley et al., 2013; Goldberger et al., 2006), reporting that HRV may act as a physiomaer of cardiac wellness during post-exercise periods.

The superiority of recovery HRV over active HR and BR features is likely explained by several physiological mechanisms. First, the short duration of the 3-min CRSST is likely insufficient for participants to reach a steady-state metabolic condition, meaning that heart rate and breathing rate during activity primarily reflect

transient acceleration kinetics rather than stabilized physiological responses. Second, while exercise induces a generalized sympathetic activation, the recovery period captures parasympathetic (vagal) reactivation and the restoration of autonomic homeostasis. Systemic inflammation is known to impair vagal reactivation, making post-exercise HRV a sensitive marker of inflammatory burden and autonomic resilience. Consequently, HRV during recovery acts as a functional autonomic “stress test”, providing greater discriminatory power than short-duration activity signals (Koeneman et al., 2021). Finally, heart rate outperformed breathing rate during activity because heart rate responds rapidly to neural vagal withdrawal, whereas breathing rate is driven by slower chemoreflex mechanisms related to carbon dioxide accumulation. As a result, the heart rate signal is more physiologically mature at the end of the activity period, although still less informative than post-exercise HRV.

TABLE 6 Model performance results based on feature sources during activity and recovery periods.

Period	Features	MSE	Sensitivity	Specificity	Precision	AUC
Combined	All	0.08 (0.06)	0.38 (0.41)	0.92 (0.14)	0.67 (0.47)	0.65 (0.25)
Activity	BR	0.14 (0.12)	0.00 (0.00)	0.72 (0.27)	0.00 (0.00)	0.36 (0.13)
	HR	0.07 (0.07)	0.47 (0.45)	0.85 (0.20)	0.67 (0.24)	0.66 (0.23)
	MV	0.11 (0.09)	0.10 (0.20)	0.90 (0.20)	0.50 (0.50)	0.50 (0.16)
Recovery	BR	0.14 (0.16)	0.00 (0.00)	0.84 (0.20)	0.00 (0.00)	0.43 (0.10)
	HR	0.10 (0.11)	0.40 (0.49)	0.80 (0.24)	0.62 (0.12)	0.60 (0.12)
	MV	0.10 (0.09)	0.50 (0.45)	0.88 (0.14)	0.62 (0.41)	0.69 (0.26)
	HRV	0.13 (0.14)	0.70 (0.40)	0.77 (0.29)	0.75 (0.25)	0.73 (0.16)

Abbreviations: BR (breathing rate), HR (heart rate), MV (minute ventilation), HRV (heart rate variability), MSE (mean squared error), AUC (area under the curve). Highest AUC per period (activity, recovery) shown in bold. Metrics are reported as mean (standard deviation).

TABLE 7 Most important features identified by the model, ranked by their relative importance scores.

Feature name	Feature importance
lf_hf_ratio	0.174
std_hr	0.172
peaks	0.167
n_above_mean	0.142
skewness	0.123
range_nni	0.095
kurtosis	0.067
mean_nni	0.059

4.4 Effect of binary conversion threshold on model performance

Our study design allows setting a binary conversion threshold to the IRS. An additional exploratory objective was to assess the effect of varying the threshold level on model performance. This analysis confirms that the most balanced tradeoff between high sensitivity and specificity is attained when setting a threshold of 0. Other threshold values result in either higher sensitivity or specificity. This approach enables flexibility in adjusting the sensitivity and specificity of the model and it becomes particularly significant when considering the real-world implementation of our models in different scenarios and settings. The choice of the threshold should align with the specific objectives of the given context, taking into account the desired outcome and priorities.

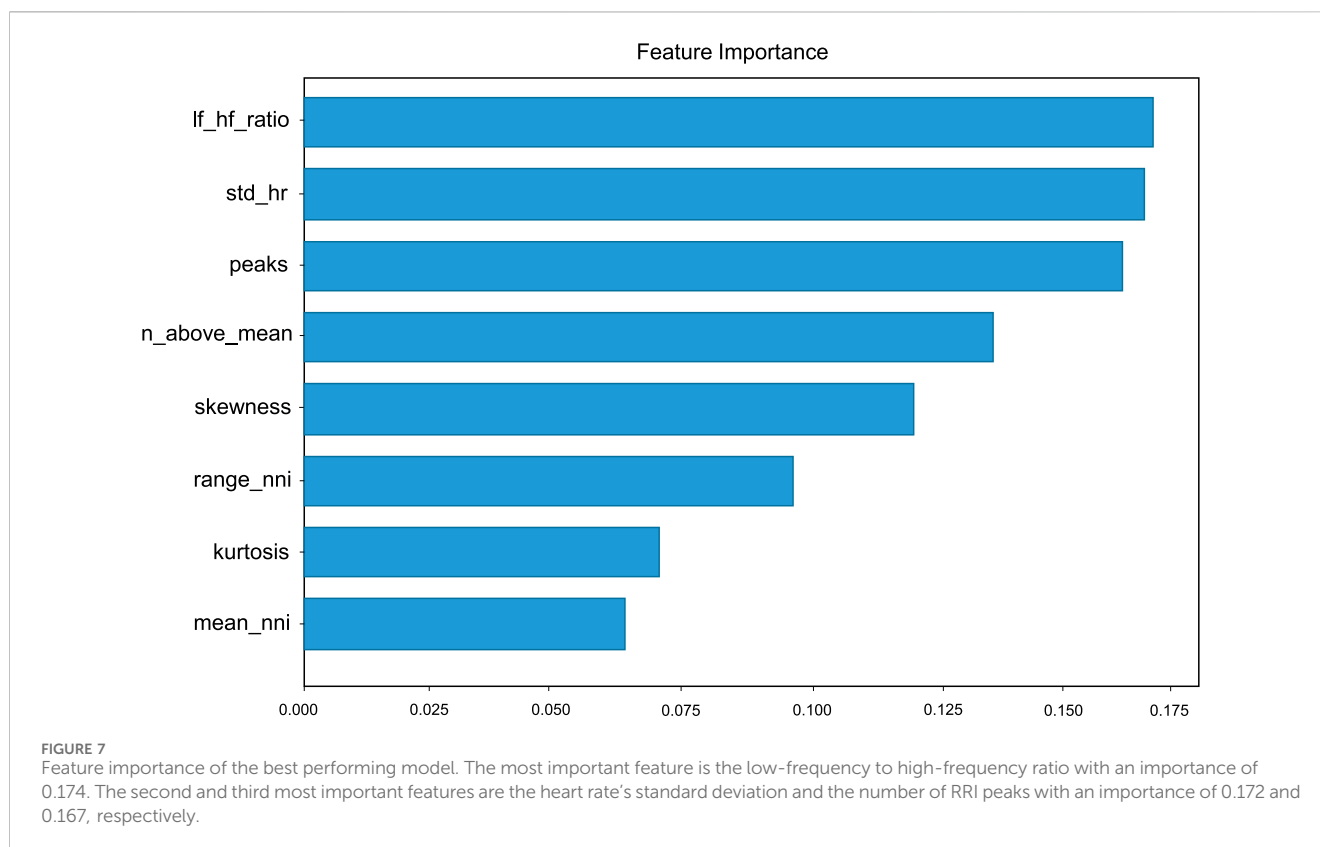
4.5 Comparison with previous studies

Our results are not directly comparable to existing studies due to the uniqueness of our approach, which not only includes measurement of inflammatory biomarkers in blood samples, but also changes in cardiac and respiratory variables during a controlled physiological stress, i.e., 3-min CRSST. It must be regarded that

variations in approaches, methodologies, features, and objectives between the studies have an impact and should be taken into consideration. Most studies relied on patient-reported diagnoses rather than quantitative measurements of inflammatory markers to predict VRTIs. In the previous iteration of our study (Hadid et al., 2025), we enrolled 55 healthy adults who continuously wore up to three different wearable devices (Oura ring, Astroskin–Hexoskin shirt, Biobeat watch), yielding more than 52,000 inflammatory biomarker datapoints from 1001 blood samples. Following inoculation, 78% of participants developed systemic inflammation, which allowed us to establish an objective ground truth for model development. The resulting dataset comprised 582 post-cleaning events, of which 18% were classified as inflamed based on an individualized coefficient of variance threshold. Physiological responses were observed as early as 12–24 h post-inoculation, and inflammatory surges peaked between 36 and 72 h. Using this rich biomarker-anchored dataset, we developed and tested eight wearable-based models. Our candidate model, relying on a minimal feature set from the Oura ring during sleep, achieved a ROC-AUC of 0.73 (95% CI 0.71–0.74) in real-time prediction and 0.89 (0.87–0.90) in the 24h-tolerance analysis (Hadid et al., 2025). In the context of VRTIs caused by COVID-19, Quer et al. (Quer et al., 2020) reported an AUC of 0.72 when relying on resting heart rate, sleep, and activity metrics. Mason et al. (Mason et al., 2022) and Conroy et al. (Conroy et al., 2022) achieved AUCs of 0.82 with sensitivity of 82% and 62% and specificity of 63% and 88%, respectively. Our model in this study shows slightly lower performance compared to these studies (AUC of 0.73 in real-time), but it is important to note that our results were achieved using objectively validated biomarkers rather than symptom reports (Hadid et al., 2025). Moreover, our classification of inflammation versus non-inflammation likely precedes symptom onset, suggesting a higher value for proactive monitoring in public-health and early-warning applications.

4.6 Limitations

Several limitations are worth noting. The 3-min CRSST was performed under controlled laboratory conditions. The 3-min CRSST was also performed at a fixed rate of 30 steps/min. While



the step rate is fixed/constant across all participants, the level of physiological stress will vary between based on their age, sex, cardiorespiratory fitness and body mass. The CRSST is simple and requires minimal equipment (a single 20 cm step and a pacing device) making it feasible to perform in homes or workplaces with wearable monitoring; however, variations in step execution or cadence outside the lab could affect physiological responses. Future studies should evaluate model performance in these real-world conditions. Potential participants could reproduce this task in real-world settings, but the quality of task execution may affect the performance of our algorithms. Ideally, strenuous physical activity (and recovery) would be automatically detected using the wearable devices and algorithms would be robust enough to perform under these types of uncontrolled activities. This makes further investigations imperative for validating these findings in diverse settings that account for representing real-world conditions. In addition, missing and noisy data led to a reduction in the dataset size. The utilization of consumer-grade wearable devices (smaller and more convenient for every-day use compared to the Astroskin that comes with a head band and requires the user to put a relatively large device measuring the acceleration in the correct orientation) for data collection, while not eliminating the possibility of recording missing and noisy data, would allow for more extensive data collection to be conducted. Furthermore, the group of participants in our study was limited since we specifically focused on healthy adults. It is important to recognize that extending our conclusions to groups like the elderly or vulnerable populations may require additional investigation. These groups may exhibit variations in their physiological responses to infections, exercise, and unique profiles of biomarker changes.

Additionally, It is important to note that individual differences in physical fitness and lifestyle factors, such as caffeine consumption, may influence physiological responses during the stair-stepping test. Further, participants with significant mobility limitations were excluded, and therefore our findings are not generalizable to individuals who are unable to perform such exercise tasks. Future studies could incorporate stratification by fitness level, standardized dietary controls, and alternative exercise or passive monitoring protocols to expand applicability. Consequently, future research should aim to replicate and adapt our methodology to these diverse populations, ensuring broader applicability and effectiveness of our early detection approach. Finally, it is essential to recognize the limitations of our study concerning the specificity of detectable inflammations. Our emphasis on respiratory inflammation and specific biomarkers associated with this context may not encompass the full spectrum of inflammatory responses within the body. Inflammatory processes can vary significantly depending on underlying causes and affected systems. While our model displays promise in detecting systemic inflammatory surges due to viral respiratory tract infections, its specificity may be more confined to this particular inflammatory context. Researchers should exercise caution when applying our findings to broader inflammatory conditions, considering the need for context-specific models in such cases.

Several strategies could be employed to address the limitations identified in this study. Future work could stratify participants by fitness level, standardize dietary and caffeine intake, and record environmental or seasonal factors. Alternative exercise protocols or passive monitoring could enable inclusion of participants with mobility limitations.

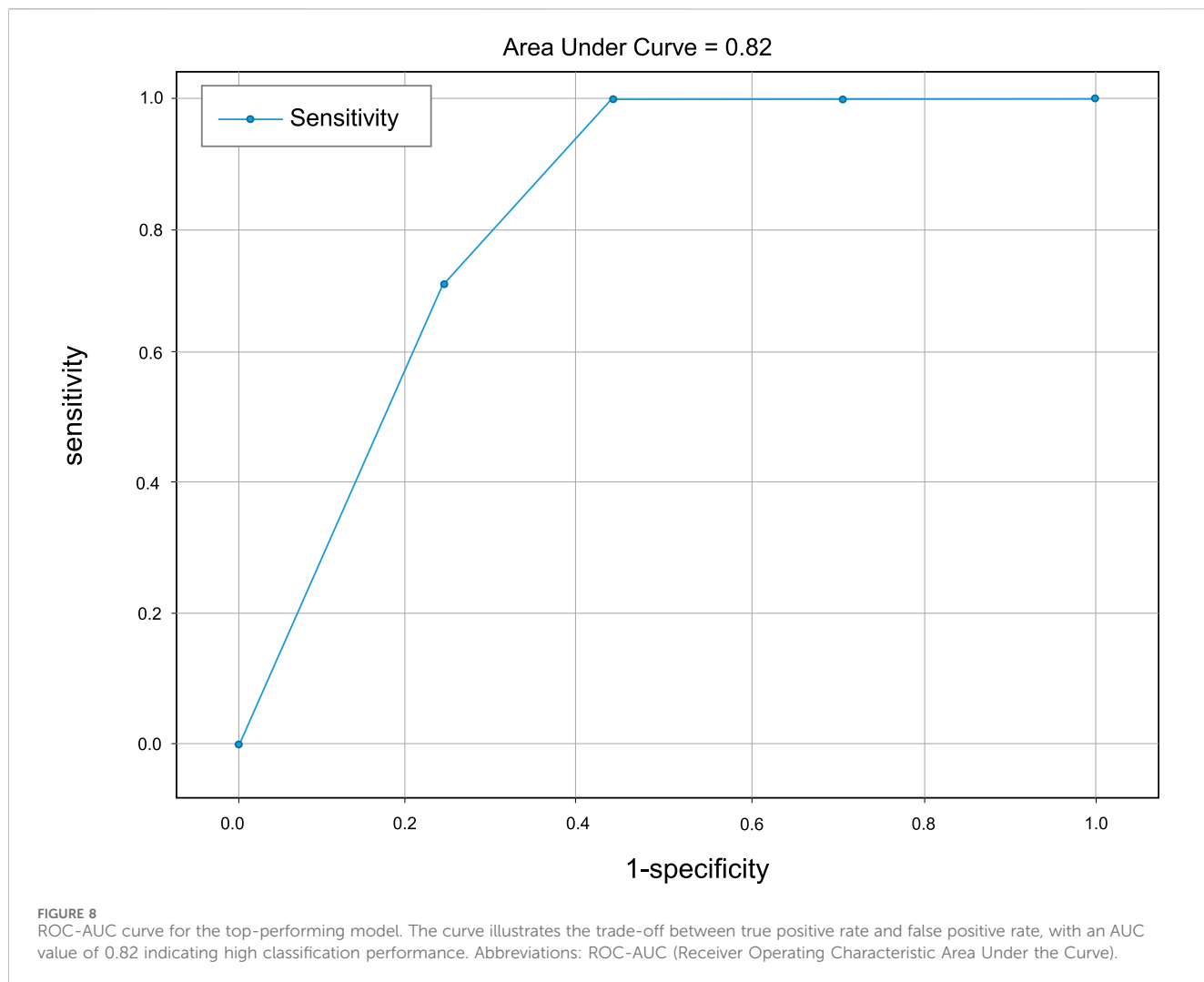


TABLE 8 Effect of varying the decision threshold on sensitivity, specificity, and the number of true positives and true negatives.

Threshold	Sensitivity	Specificity	True positives (visits)	True negatives (visits)
-0.3	1.00	0.00	16	0
-0.2	1.00	0.30	7	2
-0.1	1.00	0.57	7	5
0	0.70	0.77	5	7
0.1	0.00	0.83	0	11
0.2	0.00	0.83	0	11
0.3	0.00	1.00	0	15

5 Conclusion

The findings validate the effectiveness of wearable biosensors and machine-learning techniques for early detection of VRTIs. By analyzing physiological variables, particularly heart rate variability (HRV) and their changes during a controlled physiological stress

and recovery protocol (3-min CRSST), the model demonstrated notable accuracy in predicting inflammation levels associated with the onset of respiratory infections. This highlights the value of integrating quantitative physiological measurements and advanced data analysis approaches in healthcare settings. The study's outcomes have significant implications for public health,

as early detection based on stress-response dynamics can enable timely intervention and help mitigate future outbreaks.

6 Data sharing

De-identified data and code may be available for educational or research purposes upon reasonable request to the Principal Investigator Dennis Jensen (dennis.jensen@mcgill.ca), subject to interinstitutional data sharing agreements.

7 Equations

$$IRS = \frac{1}{n} \sum_{i=1}^n x_i \quad (1)$$

where:

n = Number of measured biomarkers (8)
 x_i = Individual biomarker measurement at index i

$$CoV = \left(\frac{\sqrt{\frac{1}{n} \sum_{i=1}^n (X_i - \bar{X})^2 + \frac{1}{n} \sum_{i=1}^n (Y_i - \bar{Y})^2}}{\frac{1}{n} \sum_{i=1}^n X_i + \frac{1}{n} \sum_{i=1}^n Y_i} \right) \quad (2)$$

where:

X_i = IRS values at the first baseline visit ($i = 1, 2$)
 Y_i = IRS values at the second baseline visit ($i = 1, 2$)
 \bar{X} = Mean of the IRS values at the first visit
 \bar{Y} = Mean of the IRS values at the second visit
 n = Number of IRS values (pairs of values)

$$\text{Normalized IRS} = IRS - \text{average CoV} - 1 \quad (3)$$

$$f = \sum_{i=1}^5 x_i - \sum_{j=1}^5 (x-1)_j \quad (4)$$

where:

f = The calculated feature
 x_i = Last 5 data points in minute x
 $(x-1)_j$ = First 5 data points in minute $x-1$

$$\text{Feature Importance} = \frac{\text{Sum of Gains for All Splits on a Feature}}{\text{Total Sum of Gains in the Model}} \quad (5)$$

Data availability statement

The raw data supporting the conclusions of this article will be made available by the authors, without undue reservation.

Ethics statement

The Research Institute of the McGill University Health Centre approved the study (WE SENSE/2022-7591). The studies were conducted in accordance with the local legislation and institutional requirements. The participants provided their written informed consent to participate in this study.

Author contributions

OJ: Validation, Methodology, Visualization, Data curation, Investigation, Writing – review and editing, Conceptualization, Software, Writing – original draft. AH: Supervision, Conceptualization, Methodology, Investigation, Writing – review and editing. EM: Writing – review and editing, Resources, Conceptualization, Supervision. QD: Data curation, Software, Writing – review and editing. CP: Data curation, Writing – review and editing. AT: Data curation, Writing – review and editing. MC: Writing – review and editing, Investigation. JP: Writing – review and editing, Conceptualization. ML: Writing – review and editing, Conceptualization. DJ: Writing – review and editing. PD: Writing – review and editing, Formal Analysis, Supervision, Investigation, Software, Methodology, Resources, Conceptualization.

Funding

The author(s) declared that financial support was received for this work and/or its publication. This work was supported by the Canadian Institutes of Health Research (202104PJT-462744-PH3-CFAC-143248) paid to the Research Institute of the McGill University Health Centre.

Conflict of interest

The author(s) declared that this work was conducted in the absence of any commercial or financial relationships that could be construed as a potential conflict of interest.

Generative AI statement

The author(s) declared that generative AI was used in the creation of this manuscript. During the preparation of this work the author(s) used ChatGPT 4-o in order to proofread the language. After using this tool/service, the author(s) reviewed and edited the content as needed and take(s) full responsibility for the content of the published article.

Any alternative text (alt text) provided alongside figures in this article has been generated by Frontiers with the support of artificial intelligence and reasonable efforts have been made to ensure accuracy, including review by the authors wherever possible. If you identify any issues, please contact us.

Publisher's note

All claims expressed in this article are solely those of the authors and do not necessarily represent those of their affiliated organizations, or those of the publisher, the editors and the reviewers. Any product that may be evaluated in this article, or claim that may be made by its manufacturer, is not guaranteed or endorsed by the publisher.

References

- Blackie, S. P., Fairbairn, M. S., McElvaney, N. G., Wilcox, P. G., Morrison, N. J., and Pardy, R. L. (1991). Normal values and ranges for ventilation and breathing pattern at maximal exercise. *Chest* 100, 136–142. doi:10.1378/chest.100.1.136
- Boullousa, D. A., Barros, E. S., del Rosso, S., Nakamura, F. Y., and Leicht, A. S. (2014). Reliability of heart rate measures during walking before and after running maximal efforts. *Int. J. Sports Med.* 35 (12), 999–1005. doi:10.1055/s-0034-1372637
- Carter, N., and Curran, M. (2011). Live attenuated influenza vaccine (flumist®; fluenztm). *Drugs* 71 (12), 1591–1622. doi:10.2165/11206860-000000000-00000
- Chen, T., and Guestrin, C. (2016). “Xgboost: a scalable tree boosting system,” in *Proceedings of the 22nd ACM SIGKDD international conference on knowledge discovery and data mining, KDD '16* (New York, NY, USA: Association for Computing Machinery), 785–794. doi:10.1145/2939672.2939785
- Chi, Y., Zhu, Y., Wen, T., Cui, L., Ge, Y., Jiao, Y., et al. (2013). Cytokine and chemokine levels in patients infected with the novel Avian influenza A (H7N9) virus in China. *J. Infect. Dis.* 208 (12), 1962–1967. doi:10.1093/infdis/jit440
- Conroy, B., Silva, I., Mehraei, G., Damiano, R., Gross, B., Salvati, E., et al. (2022). Real-time infection prediction with wearable physiological monitoring and AI to aid military workforce readiness during COVID-19. *Sci. Rep.* 12, 3797. doi:10.1038/s41598-022-07764-6
- Davey, R. J., Lynfield, R., Dwyer, D., Losso, M. H., Cozzi-Lepri, A., Wentworth, D., et al. (2013). The association between serum biomarkers and disease outcome in influenza A (H1N1)pdm09 virus infection: results of two international observational cohort studies. *PLOS ONE* 8 (2), e57121. doi:10.1371/journal.pone.0057121
- Developers, N. (2025). Numpy.trapz. Available online at: <https://numpy.org/doc/1.25/reference/generated/numpy.trapz.html> (Accessed on October 16, 2025).
- Elsaid, W. S. I. M. (2011). *Evaluating the validity and reliability of harvard step test to predict vo2max in terms of the step height according to the knee joint angle, theories and Applications the international edition*, 1, 126–132. Available online at: https://jassalexu.journals.ekb.eg/article_84908_ffb5d991ba49a1d3f2c21865a9bf679.pdf.
- Farooq, K., Lim, M., Dennison-Hall, L., Janson, F., Olszewska, A. H., Ahmad Zabidi, M. M., et al. (2024). Evaluation of machine learning to detect influenza using wearable sensor data and patient-reported symptoms: cohort study. *J. Med. Internet Res.* 26, e48779. doi:10.2196/47879
- Foll, S., Maritsch, M., Spinola, F., Mishra, V., Barata, F., Kowatsch, T., et al. (2021). Flirt: a feature generation toolkit for wearable data. *Comput. Methods Programs Biomed.* 212, 106461. doi:10.1016/j.cmpb.2021.106461
- Goldberger, J. J., Le, F. K., Lahiri, M., Kannankeril, P. J., Ng, J., and Kadish, A. H. (2006). Assessment of parasympathetic reactivation after exercise. *Am. J. Physiology - Heart Circulatory Physiology* 290, H2446–H2452. doi:10.1152/ajpheart.01118.2005
- Haarala, A., Kahonen, M., Eklund, C., Jylhava, J., Koskinen, T., Taittonen, L., et al. (2011). Heart rate variability is independently associated with C-reactive protein but not with serum amyloid A. the cardiovascular risk in young finns study. *Eur. J. Clin. Investigation* 41 (9), 951–958. doi:10.1111/j.1365-2362.2011.02485.x
- Hadid, A., McDonald, E. G., Cheng, M. P., Papenburg, J., Libman, M., Dixon, P. C., et al. (2023). The sense study protocol: a controlled, longitudinal clinical trial on the use of wearable sensors for early detection and tracking of viral respiratory tract infections. *Contemp. Clin. Trials* 128, 107103. doi:10.1016/j.cct.2023.107103
- Hadid, A., McDonald, E. G., Ding, Q., Philipp, C., Trotter, A., Dixon, P. C., et al. (2025). Development of machine learning prediction models for systemic inflammatory response following controlled exposure to a live attenuated influenza vaccine in healthy adults using multimodal wearable biosensors in Canada: a single-centre, prospective controlled trial. *Lancet Digital Health* 7 (7), 100886. doi:10.1016/j.landig.2025.100886
- Harbour, E., Lasshofer, M., Genitrini, M., and Schwameder, H. (2021). Enhanced breathing pattern detection during running using wearable sensors. *Sensors (Basel)* 21 (16), 5606. doi:10.3390/s21165606
- Hasty, F., García, G., Dávila, C. H., Wittels, S. H., Hendricks, S., and Chong, S. (2021). Heart rate variability as a possible predictive marker for acute inflammatory response in COVID-19 patients. *Mil. Med.* 86 (1–2), e34–e38. doi:10.1093/milmed/usaa405
- Inc, C. T. (2023). Hexoskin API documentation: datatype resource. Available online at: <https://api.hexoskin.com/docs/resource/datatype/> (Accessed on July 05, 2023).
- Kannankeril, P., Le, F., Kadish, A., and Goldberger, J. (2004). Parasympathetic effects on heart rate recovery after exercise. *J. Investigative Med.* 52 394–401. doi:10.1136/jim-52-06-34
- Kawamoto, S., Morikawa, Y., and Yahagi, N. (2024). Novel approach for detecting respiratory syncytial virus in pediatric patients using machine learning models based on patient-reported symptoms: model development and validation study. *JMIR Form. Res.* 8, e52412. doi:10.2196/52412
- Kieu, N. T. V., Jung, S. J., Shin, S. W., Jung, H. W., Jung, E. S., Won, Y. H., et al. (2020). The validity of the YMCA 3-minute step test for estimating maximal oxygen uptake in healthy Korean and Vietnamese adults. *J. Lifestyle Med.* 10 (1), 21–29. doi:10.15280/jlm.2020.10.1.21
- Koenen, M., Koch, R., van Goor, H., Pickkers, P., Kox, M., and Bredie, S. (2021). Wearable patch heart rate variability is an early marker of systemic inflammation during experimental human endotoxemia. *Shock* 56 (4), 537–543. doi:10.1097/shk.0000000000001827
- Lee, N., Wong, C., Chan, P., Chan, M. C. W., Wong, R. Y. K., Lun, S. W. M., et al. (2011). Cytokine response patterns in severe pandemic 2009 H1N1 and seasonal influenza among hospitalized adults. *PLOS ONE* 6 (10), e26050. doi:10.1371/journal.pone.0026050
- Lee, O., Lee, S., Kang, M., Mun, J., and Chung, J. (2019). Prediction of maximal oxygen consumption using the young men's Christian association-step test in Korean adults. *Graefes's Archive Clin. Exp. Ophthalmol.* 119 (5), 1245–1252. doi:10.1007/s00421-019-04115-8
- Lewthwaite, H., and Jensen, D. (2021). Multidimensional breathlessness assessment during cardiopulmonary exercise testing in healthy adults. *Eur. J. Appl. Physiology* 121 (2), 499–511. doi:10.1007/s00421-020-04537-9
- Lewthwaite, H., Koch, E. M., Ekström, M., Hamilton, A., Bourbeau, J., Maltais, F., et al. (2020). Predicting the rate of oxygen consumption during the 3-minute constant-rate stair stepping and shuttle tests in people with COPD. *J. Thorac. Dis.* 12 (5). doi:10.21037/jtd.2020.03.13
- Li, F., Chang, C.-H., Chung, Y.-C., Wu, H. J., Kan, N. W., ChangChien, W. S., et al. (2021). Development and validation of 3 min incremental step-in-place test for predicting maximal oxygen uptake in home settings: a submaximal exercise study to assess cardiorespiratory fitness. *Int. J. Environ. Res. Public Health* 18 (20), 10750. doi:10.3390/ijerph182010750
- Li, H., Gerkin, R. C., Bakke, A., Norel, R., Cecchi, G., Laudamiel, C., et al. (2023). Text-based predictions of COVID-19 diagnosis from self-reported chemosensory descriptions. *Commun. Med.* 3 (1), 104. doi:10.1038/s43856-023-00334-5
- Lu, S., Lin, S., Zhang, H., Liang, L., and Shen, S. (2021). Methods of respiratory virus detection: advances towards point-of-care for early intervention. *Micromachines (Basel)* 6, 697. doi:10.3390/mi12060697
- Mason, A., Hecht, F. M., Davis, S. K., Natale, J. L., Hartogensis, W., Damaso, N., et al. (2022). Detection of COVID-19 using multimodal data from a wearable device: results from the first tempredict study. *Sci. Rep.* 12, 3463. doi:10.1038/s41598-022-07314-0
- Mayeux, R. (2004). Biomarkers: potential uses and limitations. *NeuroRx* 2, 182–188. doi:10.1602/neurorx.1.2.182
- McClain, M. T., Henao, R., Williams, J., Nicholson, B., Veldman, T., Hudson, L., et al. (2015). Differential evolution of peripheral cytokine levels in symptomatic and asymptomatic responses to experimental influenza virus challenge. *Clin. Exp. Immunol.* 183 (3), 441–451. doi:10.1111/cei.12736
- Monteerarat, Y., Sakabe, S., Ngamurult, S., Srichathaphimuk, S., Jiamtom, W., Chaichuen, K., et al. (2010). Induction of TNF α in human macrophages by avian and human influenza viruses. *Archives Virology* 155 (8), 1273–1282. doi:10.1007/s00705-010-0716-y
- Montes, J., Young, J., Tandy, R., and Navalta, J. W. (2018). Reliability and validation of the hexoskin wearable bio-collection device during walking conditions. *Int. J. Exerc. Sci.* 11 (7), 806–816. doi:10.70252/YPHF4748
- Narin, A., Kaya, C., and Pamuk, Z. (2021). Automatic detection of coronavirus disease (COVID-19) using X-ray images and deep convolutional neural networks. *Pattern Analysis Appl.* 24 (3), 1207–1220. doi:10.1007/s10044-021-00984-y
- of Canada, G. (2023). COVID-19 epidemiology update: current situation. Available online at: <https://health-infobase.canada.ca/covid-19/current-situation.html#graphHospVentICU> (Accessed on June 02, 2023).
- Peiris, J., Yu, W., Leung, C., Cheung, C. Y., Ng, W. F., Nicholls, J. M., et al. (2004). Re-emergence of fatal human influenza A subtype H5N1 disease. *Lancet* 363 (9409), 617–619. doi:10.1016/S0140-6736(04)15595-5
- Quer, G., Radin, J. M., Gadaleta, M., Baca-Motes, K., Ariniello, L., Ramos, E., et al. (2020). Wearable sensor data and self-reported symptoms for COVID-19 detection. *Nat. Med.* 27, 73–77. doi:10.1038/s41591-020-1123-x
- Shen, M., Zhou, Y., Ye, J., Al-Maskri, A., Kang, Y., Zeng, S., et al. (2020). Recent advances and perspectives of nucleic acid detection for coronavirus. *J. Pharm. Analysis* 10 (2), 97–101. doi:10.1016/j.jpha.2020.02.010
- Smith, C., Chillrud, S., Jack, D., Kinney, P., Yang, Q., and Layton, A. M. (2019). Laboratory validation of hexoskin biometric shirt at rest, submaximal exercise, and maximal exercise while riding a stationary bicycle. *J. Occup. Environ. Med.* 61 (4), e104–e111. doi:10.1097/JOM.0000000000001537
- Stanley, J., Peake, J. M., and Buchheit, M. (2013). Cardiac parasympathetic reactivation following exercise: implications for training prescription. *Sports Med.* 43, 1259–1277. doi:10.1007/s40279-013-0083-4
- Timothy, M., McKinley, P. S., Seeman, T. E., Choo, T.-H., and Lee, S. (2015). Heart rate variability predicts levels of inflammatory markers: evidence for the vagal anti-inflammatory. *Brain, Behav. Immun.* 49, 94–100. doi:10.1016/j.bbi.2014.12.017
- Williams, D., Keonig, J., Carnevali, L., Sgoifo, A., Jarczok, M. N., Sternberg, E. M., et al. (2019). Heart rate variability and inflammation: a meta-analysis of human studies. *Brain, Behav. Immun.* 80, 219–226. doi:10.1016/j.bbi.2019.03.009